

Detection of hydrate plugs inside submarine pipelines using neutrons

Sophie Bouat^{*a}, Ludovic Pinier^b, Xavier Sebastian^b, Adrian Losko^c, Rudolf Schütz^c, Michael Schulz^c, Zsolt Revay^c, Zeljko Ilic^{c,d,f}, Eric Mauerhofer^e, Thomas Brückel^{e,f} and Ralph Gilles^c

^a Science-SAVED, 310 impasse Sansaret, 38 410 Grenoble, France; ^b TechnipFMC, 6/8 allée de l'Arche, 92 973 Paris La Défense, France; ^c Heinz Maier-Leibnitz Zentrum (MLZ), TU München, Lichtenbergstr. 1, 85748 Garching, Germany; ^d Jülich Centre for Neutron Science (JCNS-4) at MLZ, Forschungszentrum Jülich GmbH, Garching, Germany; ^e Jülich Centre for Neutron Science (JCNS-2), Peter Grünberg Institut (PGI-4) Forschungszentrum Jülich GmbH, Jülich, Germany; ^f RWTH Aachen University, Lehrstuhl für Experimentalphysik IVc, 52056 Aachen, Germany.

*Corresponding author: Sophie BOUAT, CEO of Science-SAVED,
contact@science-saved.com, science.saved@gmail.com

Revised after last comments from the editors and Reviewers

Detection of hydrate plugs inside submarine pipelines using neutrons

Abstract: The objective of this study was to demonstrate the feasibility of localizing and detecting hydrate plugs inside submarine pipelines in situ and contactless using neutron-induced analytical techniques. Cold and fast neutron-beam instruments at Heinz Maier-Leibnitz Centre (MLZ) were used to show that neutrons penetrate through the thick wall and the insulation of such pipes and even the induced gamma radiation can be detected outside to perform a non-destructive chemical analysis within the pipe. It was found that the change in the hydrogen concentration caused by a possible hydrate plug can be detected in seconds; while with a detailed analysis at a given spot lasting for a few hours it is possible to unambiguously identify the hydrate phase inside the hydrocarbon phase.

Keywords: hydrocarbon, hydrate, submarine pipeline, neutron radiography, fast-neutron-induced gamma-ray spectrometry, prompt gamma activation analysis

Introduction

Pipelines laid on the seabed are like arteries for offshore oil and gas transportation. Due to their key role in the exploitation of offshore oil and gas resources, many studies are devoted to them [1], [2], [3], [4]. They are subjects to a large variety of damages and defects [5], [6], [7]. One of the most important operational challenges is to manage the risk of formation of gas-hydrate plugs inside the pipeline [8], [9], [10], [11].

High-pressure hydrocarbons are transported in these submarine pipelines in liquid form. At the low temperatures typical at seabed, condensed water and the hydrocarbons might form solid hydrates (see Figure 1) that block the flow. Locating and eliminating such plugs is of the highest importance in order to reactivate the pipelines. Locating them must be performed non-destructively and *in operando* since the pipeline cannot be opened or removed from the seafloor. The more commonly used techniques for hydrate detection in the oil and gas industry are thermal imaging and gamma ray

detection, but they are restricted to observation in the air and cannot be used in sea water [12]. Ultrasonic techniques are widely used in oil and gas industry [13]. Ultrasonic measurement was found to be useful also in locating the hydrate phase in hydrocarbon phase, as the ultrasound waves are reflected from the phase boundaries. The signal strength is proportional to the density difference, and the densities of the liquid hydrocarbon and the solid hydrate are close to each other, at least when hydrate is beginning to form [14], [15], [16]. Hence, the ultrasonic measurements led to a limited sensitivity: the detection of a hydrate thickness of min. 50 mm only near the pipeline wall [is possible](#) [17] and the beginning of the hydrate formation [cannot be detected](#), when it mixes with water as slurry and there is no sharp boundary between the phases. Moreover, the instrument has to be in contact with the pipeline to do such a ultrasonic detection [17], which represents another limitation since the contact with deep underwater pipelines may not be possible because of silt deposit on the pipes on the sea floor.

At the same time, the chemical compositions of the pure hydrocarbon and that mixed with water are highly different. Therefore, we were looking for contactless analytical techniques, which can analyze light elements nondestructively and both the in-going and the out-coming radiations can penetrate through the thick walls of the pipe. A nuclear analytical technique called Prompt Gamma Activation Analysis (PGAA) seemed to be suitable for our purpose, as the technique is sensitive to hydrogen even down to the ppm level [giving a strong characteristic peak at 2.223 MeV](#) [18]. PGAA is also nondestructive and it is based on the detection of characteristic gamma radiation induced by neutron irradiation.

A Remotely Operated Vehicle (ROV) carrying a neutron generator and a gamma detector was already used in the past to analyze objects lying on the sea floor [19].

Such neutron generators produce a neutron fluence of 10^{10} – 10^{12} s⁻¹ which is suitable for this application, especially since they produce more penetrable neutrons with the energy of 14 MeV [20].

[Figure 1 near here]

The feasibility studies were performed at the different cold- and fast-neutron instruments of Heinz Maier-Leibnitz Zentrum (MLZ). It was tested using mockup samples (water, oil, rubber) whether the significantly different hydrogen contents and the H-to-C ratios can be differentiated between, even through metal walls, using cold neutrons at the PGAA instrument. Due to the higher reaction cross sections of cold neutrons, PGAA allows for the measurement of small samples with volumes of a few cm³ [21].

The real pipe samples were measured in a fast neutron beam. The neutron transmission through a pipe wall was determined with fast-neutron radiography at the instrument NECTAR (Neutron Computerized Tomography and Radiography) at MLZ [22], verifying that sufficient neutrons are available inside the pipe, as was clearly shown with the FaNGaS (Fast-Neutron-induced Gamma Spectrometry) instrument, too [23]. FaNGaS was also used for chemical analysis of mockup samples inside the real-sized pipe pieces.

Materials and methods

Pipeline models

A mockup was cut from an actual commercial pipeline with the outer diameter of 428.5 mm, a length of 400 mm and a weight of about 60 kg. As shown in Figure 2, this half pipe is made of steel with the wall thickness of 20.65 mm coated with 92 mm of syntactic polypropylene that is made of classic porous polypropylene ((C₃H₆)_n) filled

with 23.9% SiO₂ micro-spheres to improve its mechanical properties [24]. Simple samples were also prepared: a couple of centimeter thick layers of steel or lead, oil, and water, and were placed in the beam or in front of the detector.

[Figure 2 near here]

Hydrocarbon and hydrate phases

The two phases of hydrocarbon and hydrate have different compositions:

- The liquid hydrocarbon phase is mainly composed of hydrocarbon molecules with traces of water molecules (see Figure 3-a) originating from condensation.
- In the solid hydrate phase, water molecules are arranged in so-called ice cages each of which traps one hydrocarbon molecule (see Figure 3-b).

Assuming methane (CH₄) as the hydrocarbon, the H-to-C molar ratio changes from 4 to 16, when the liquid phase solidifies with hydrate formation. These materials were not available for the lab experiment, so they were replaced with compounds with similar compositions.

[Figure 3 near here]

Neutron-based techniques

All neutron experiments were performed at the Heinz Maier-Leibnitz Zentrum using the FRM II research reactor [26]. It is one of the most powerful and advanced neutron sources in the world. With the help of nuclear fission, more than 10¹⁴ free neutrons per square centimeter and second are produced for research, industry and medicine. The thermal power adds up to 20 MW. In our experiments, fast (0.1–10 MeV) and cold (~5 meV) neutrons were used. The fast neutrons are produced in a converter containing enriched uranium, while the cold neutron beam originates from the

cold source filled with liquid deuterium moderating the thermal neutrons of the reactor tank.

Besides the imaging, two nuclear analytical techniques were used in this series of experiments; both of them are based on the detection of neutron-induced gamma radiations. PGAA is a precisely calibrated instrument, where we could directly derive the H-to-C molar ratios from the peak-area ratios, and it could be compared with the real molar ratios. FaNGaS is still in experimental state, the analytical sensitivities of the characteristic lines are not yet determined. So FaNGaS was used for large, real samples (pipes) and to check if the change of the H signal and H/C ratio could be monitored, when the H content changed inside the pipe.

Fast Neutron Radiography with the NECTAR instrument

To test the feasibility of fast-neutron-based techniques, the neutron transmission through a pipe wall was studied with fast-neutron radiography at the instrument NECTAR. The nearly parallel fast-neutron beam is directed on the sample, behind which a scintillator screen converts the neutrons to visible light detected by an optical system [22]. The flux of the fast neutron beam is about $10^8 \text{ cm}^{-2}\text{s}^{-1}$ at sample position. Spots in the image, where the sample absorbs the neutrons, remain darker, thus mapping the internal structure of the object. In this case, only the transmitted intensities were compared with and without sample in the beam. The half pipe was measured in this way.

Fast-neutron-induced gamma-ray spectrometry with the FaNGaS instrument

FaNGaS is located at the same beam port as NECTAR. The beam was collimated to the sizes of $60 \times 60 \text{ mm}^2$ and $5 \times 10 \text{ mm}^2$ according to the respective needs. The neutrons, hitting the sample, induce inelastic scattering on the atomic nuclei, during

which they become excited. The excitation energy is released in the form of characteristic gamma radiation, whose energies can be used for the identification of the emitter element, while the intensities (peak areas) are proportional to its amount. The gamma radiation was acquired using a high-purity germanium detector shielded with 15 cm of lead and 20–28 cm borated polyethylene. The gamma radiation emitted by the sample is furthermore collimated using a cylindrical lead tube with the internal diameter of 60 mm. Depending on the neutron collimator settings, approximately 160 cm³ or just 3 cm³ of the sample was analyzed in the crossing of the beam and the gamma-ray detection. The gamma spectra were evaluated with a fitting program called Hypermet-PC [26].

It needs to be mentioned that HPGe detectors must be cooled to a temperature of at least –150°C. Cooling solutions for submarine applications are available at certain manufacturers. Scintillator detectors requiring no cooling have successfully been used in similar underwater applications [18].

The following setup was applied as presented in Figure 4: A polyethylene (PE, (C₂H₄)_n) block (black in Figure 4-a) was placed in the centre of the half pipe, which was placed in such a way that both the neutrons and the detected gamma rays were attenuated, as it will be in real circumstances. An example of recorded gamma spectrum is shown in Figure 4-b.

[Figure 4 near here]

Prompt Gamma neutron Activation Analysis: PGAA

PGAA is also a non-destructive nuclear analytical technique based on the so-called radiative neutron capture, i.e. detection of characteristic gamma rays induced by the absorption of neutrons in the atomic nucleus. Using their characteristic energies, one can identify the element, while their intensities (peak areas) are proportional to the

number of nuclei of the element contained within the irradiated volume. At MLZ, PGAA is performed using a cold neutron beam, whereby the neutron flux can be adjusted to the needs of the experiment between $5 \times 10^7 \text{ cm}^{-2}\text{s}^{-1}$ and $4 \times 10^{10} \text{ cm}^{-2}\text{s}^{-1}$, but in this series of experiments the flux of $10^8 \text{ cm}^{-2}\text{s}^{-1}$ was used. The beam is collimated to the size of $20 \times 20 \text{ mm}^2$. The gamma radiation from the sample is also collimated by a cylindrical collimator with a diameter of 20 mm. Thus, approximately 8 cm^3 of the sample is analyzed in the crossing of the beam and the gamma-ray detection. The gamma spectra are evaluated with the Hypermet-PC program [27], and the ratios of various elements are then determined from the peak area ratios. The major field of application for PGAA is the analysis of light elements with special emphasis on hydrogen.

Having much higher cross sections, cold neutrons absorb in the material in a shorter path (mm-cm range), thus large object (>100 g) cannot be irradiated at the PGAA facility. Hence, the pipe and its content were simulated with smaller objects. The different H-containing materials were the following: a rubber $((\text{C}_5\text{H}_8)_n)$ block with the thickness of 3 cm, oil (approximately $(\text{CH}_2)_n$), water and NaCl solution (3.5%, “sea water”) in PE bags with the thickness of about 1 cm in the neutron beam. The gamma-ray attenuation in the pipe wall was simulated with steel sheets with the total thickness of 2 cm in front of the detector. Experiments were performed with a rubber block in the neutron beam to simulate the hydrocarbon alone, then covering it with the mentioned liquid-containing bags to alter the average hydrogen content of the sample and to simulate the submarine environment. The bags were measured individually and with the rubber to account for their individual contributions in the activation. The experimental set-up is shown in Figure 5-a (with an example of recorded PGAA spectrum in Figure 5-b).

[Figure 5 near here]

Results

Fast Neutron Radiography (at NECTAR facility)

The neutron transmission was determined to be 21% through the pipe wall. It shows that a significant number of neutrons, including scattered neutrons, make it to the core of the pipe and it means a sufficient neutron flux for the analysis.

Fast Neutron-induced Gamma Spectroscopy (FaNGaS) experiments

FaNGaS experiments were performed with the experimental setup presented in Figure 4. Recorded hydrogen and carbon peaks in the gamma spectra are shown in Figure 6.

Hydrogen has only one line at 2223 keV (see peak noted "H PGAA") which is produced by capture of neutrons moderated partly in the hydrogenous sample. Due to the presence of both thermal and fast neutrons, most elements have two reactions: neutron capture and inelastic neutron scattering. Both of them were found for carbon: the peak at 4438 keV originates from inelastic scattering (see peak noted "C FaNGaS") and it is broadened because of the Doppler effect; the prompt gamma line at 4945 keV (noted as "C PGAA", due to radiative neutron capture of carbon) is also detected with a smaller intensity. *As it can be seen, the hydrogen peak is more than two orders of magnitude stronger than the carbon peaks.*

[Figure 6 near here]

The hydrogen signal originates from two sources: from the background, i.e. it can be detected in the arrangement without a sample and from a hydrogen-containing sample. The change in the H and C signals depends on the change in the sample composition, though the compositions could not be derived directly. While the C lines

needed more than an hour to show acceptable statistics, the **strong** H signal became detectable in just a few seconds. Hence, two measurement times were used: a 5 min and a 1.5 h.

Prompt Gamma Activation Analysis (PGAA) experiments

For similar reasons, different acquisition times were used for PGAA as well. In the shorter measurements (15–60 minutes), the carbon peak reached about 1000 counts. For better statistics, a measurement was performed overnight, i.e. about 15 hours.

In the spectra, one can see the strong peak of hydrogen and the three peaks of carbon (Figure 5-b). The peak at 1260 keV is too weak to be used as a reference and the one at 3684 keV is interfering with other peaks; that is why the peak at 4945 keV was chosen as the reference C peak (especially for the calculation of H/C ratios). Other elements present in the rubber are also detected: sulphur (S) used for the rubber vulcanization and calcium (Ca) from the calcium carbonate often used to reduce the cost of rubber products.

In the first experiment, the gamma-ray attenuation of the steel wall was investigated. A rubber block was measured with and without a set of iron plates with the total thickness of 2 cm in front of the detector. One should mention, however, that neutrons scattered on hydrogen-containing samples irradiate the surrounding materials, including the steel absorber. This increases the total count rate in the spectrum also causing spectral interferences and that increases the uncertainties of the components of interest and may lead to an overload of the detector.

Then, the H/C ratios were studied for different samples. A block of rubber was used to simulate the hydrocarbon phase, with adding water to it, the appearance of the hydrate phase, and with adding oil, the mixture of hydrocarbon-hydrate phase. The H and C peaks can be seen in Figure 7-a, while the H/C peak ratios in Figure 7-b. This

result confirms that the PGAA technique is able to differentiate between samples with different H and C contents similar to those of hydrocarbon and hydrate.

[Figure 7 near here]

In the last experiment, water and salty water was used to attenuate the neutron beam. The hydrogen signal increased drastically clearly showing that the H atoms of the added water layers were partly detected. At the same time, the carbon peaks remained detectable. Thanks to the significantly different H contents of the two phases, with monitoring the H peak intensity alone, the discrimination between hydrocarbon and hydrate proved to be feasible with the possibility to follow the growth of hydrate inside the hydrocarbon phase (see Figure 8).

[Figure 8 near here]

It should be noted that during measurements with water, a special care must be taken of the geometry: it must be guaranteed that the detector does not see much of the external water which is certainly partly irradiated by the neutron source.

Discussion

Fast Neutron-induced Gamma Spectroscopy (FaNGaS) results

Table 1 presents the results: H/C intensity ratios and H peak. Based on the ratio of H and C peak intensities, the PE sample can clearly be detected inside the pipe. The difference can be quantified between its presence or absence: the H/C ratio is almost 4 times higher when this sample is present inside the pipe (see Table 1).

[Table 1 near here]

The hydrocarbon-like sample (polyethylene) could easily be detected in a few seconds: it increased the H signal 5 times (see Table 1). This result confirms that the

change in the internal hydrogen content inside a pipe can be monitored in seconds through the pipe walls.

Prompt Gamma Activation Analysis (PGAA) results

The analyses of the rubber samples reproduced the theoretical compositions independent of their thickness (see Table 2). When the rubber was measured with a steel attenuator, the ratio was found to be somewhat lower. It is caused by the iron attenuator, which absorbs the 2.2-MeV gamma radiation slightly stronger. This can be corrected for the proper counting efficiency for the given conditions.

[Table 2 near here]

The carbon peak at 4945 keV was sometimes weak, it was detectable in all cases. In the case of complex samples, the ratio depended on the order of the samples in the beam, too. The first sample always interacted with the beam before it reached the second, so the first sample's composition dominated the H/C ratio (see in Table 2, the difference between 'Water + rubber' and 'Oil + Rubber' and between 'Oil + Water' and 'Water + Oil'). This dependence allows accounting for the different compositions that could occur during the hydrate formation inside a hydrocarbon fluid. As these different compositions are easily detectable, this confirms that the PGAA technique is perfectly suited to differentiate between hydrocarbon and hydrate phases. The oil sample covered with water and "sea water" layers (Table 2), also yielded detectable carbon peaks even when using steel absorbers in front of the detector, so its ratio to hydrogen could be determined without any problem. It confirms that the internal content can be analysed with PGAA even when absorber layers cover it from all directions.

Conclusion

The experiments were performed at the Heinz Maier-Leibnitz Centre (MLZ) to decide whether hydrocarbons and their hydrates can be differentiated between in submarine pipelines using neutron-induced gamma rays. The results clearly show that under proper conditions such an analysis can be performed successfully contactless also confirming that using an on-board neutron source and a detector installed on a ROV designed for deep sea water such measurements can be performed in a reasonable amount of time. In our experiments, high-purity germanium detectors were used, but scintillator detectors are equally efficient for the detection of the strong hydrogen line. It was demonstrated that when the average hydrogen content in the pipeline shows a sudden change, which is characteristic to the appearance of the hydrate phase, it can be detected in seconds. At such locations, a more detailed analysis lasting perhaps a few hours will enable to determine the H/C ratio of the volume of interest providing more information on the formation of the hydrate phase. The experiments also showed that the hydrogen contents of the plastic insulation and the ambient water irradiated by the scattered neutrons can cause an interference with the signal of interest. Even in such cases, the composition change can be monitored. The proper measurement geometry must be determined to minimize the interferences from the background. Experiments using neutron-generator-based analytical instruments on real pipes are planned.

Acknowledgements: Industrial users would like to thank the scientists and engineers from MLZ, for arranging meetings and managing smoothly experiments flow at the Research Neutron Centre Heinz Maier-Leibnitz Zentrum in Garching near Munich.

References

- [1] Y. Ouyang, C. Wang, Y. Wu, J. Zhang, Z. Lin and L. Cai, "*Trend of the environmental supervision on submarine pipeline installation*", *Environmental Science and Pollution Research* (2018) 25, pp. 28829-28833.
- [2] B. Zhang, R. Gong, T. Wang and Z. Wang, "*Causes and Treatment Measures of Submarine Pipeline Free-Spanning*", *Journal of Marine Science and Engineering* 2020, 8, p. 329.
- [3] X. Qian and H. S. Das, "*Modeling Subsea Pipeline Movement Subjected to Submarine Debris-Flow Impact*", *Journal of Pipeline Systems Engineering and Practice* 2019, Vol. 10 (3), p. 04019016.
- [4] X. Xu, L. Wang, Z. Li, S. Yao and X. Fang, "*Modeling of submarine initial pipe-laying process and its real-time semi-physical virtual reality system*", *Advances in Mechanical Engineering* 2018, Vol. 10 (1), pp. 1-17.
- [5] C. Xiong, Z. Li, X. Sun, J. Zhai and Y. Niu, "*An Effective Method for Submarine Pipeline Inspection Using Three-Dimensional (3D) Models Constructed from Multisensor Data Fusion*", *Journal of Coastal Research* 2018, Vol. 34 (4), pp. 1009-1019.
- [6] Y. Chen, M. Gao, C. Ao, H. Liu, S. Ma and H. Liu, "*Collapse Failure of Submarine Pipelines with Corrosion Defect*", *IOP Conf. Series: Earth and Environmental Science* 332 (ICEEMS 2019) pp. 032048.
- [7] C. Coppard, A. L. Forrest, Z. Q. Leong and A. Hargrave, "*Assessment of Subsea Pipelines*", *Journal of Annual Conference of the Australasian Corrosion Association* 2014: Corrosion and Prevention 2014, Paper 78.

- [8] E. G. Hammerschmidt, "*Formation of Gas Hydrate in Natural Gas Transmission Lines*", Industrial and Engineering Chemistry 1934, Vol. 26 (8), pp. 851-855.
- [9] L. Wenqing, G. Jing, L. Xiaofang, Z. Jiankui, F. Yaorong and Y. Da, "*A study of hydrate plug formation in a subsea natural gas pipeline using a novel high-pressure flow loop*", Petroleum Science 2013, Vol. 10, pp. 97-105.
- [10] S. Zarinabadi and A. Samimi, "*Problems of Hydrate Formation in Oil and Gas Pipes Deals*", Aust. J. Basic & Appl. Sci., 5(12): 741-745 (2011).
- [11] Zainab T. Al-Sharify, Lahieb Faisal M, Luay Badr Hamad and Hussein A. Jabbar, "*A Review of Hydrate Formation in Oil and Gas Transition Pipes*", IOP Conf. Series: Materials Science and Engineering 870 (2020) 012039.
- [12] B. Chandragupthan and G. B. Nounchi, "Detecting and dealing with hydrate formation", Digital Refining – Processing, Operations & Maintenance, article 1000465 (Apr-2010), www.digitalrefining.com/article/1000465 - Gas 2010, pp 27-31, <https://cdn.digitalrefining.com/data/articles/file/67785562.pdf>.
- [13] W.M. Alobaidi, E.A. Alkuam, H.M. Al-Rizzo and E. Sandgren, "Applications of Ultrasonic Techniques in Oil and Gas Pipeline Industries: A Review", American Journal of Operations Research, 5, 274-287 (2015).
- [14] A. Sinquin, T. Palermo and Y. Peysson, "Rheological and Flow Properties of Gas Hydrate Suspensions", Oil & Gas Science and Technology – Rev. IFP, Vol. 59 (2004), No. 1, pp. 41-57.
- [15] A.A.A. Majid, D.T. Wu and C.A. Koh, "A Perspective on Rheological Studies of Gas Hydrate Slurry Properties", Engineering 4 (2018) 321–329.

- [16] P.H. de Lima Silva, M.F. Naccache, P. R. de Souza Mendes, A. Teixeira and L.S. Valim, “Rheology of THF hydrate slurries at high pressure”, *Oil & Gas Science and Technology – Rev. IFP Energies nouvelles* 75, 16 (2020).
- [17] X. Li, Y. Liu, Z. Liu, J. Chu, Y. Song, T. Yu and J. Zhao, “A hydrate blockage detection apparatus for gas pipeline using ultrasonic focused transducer and its application on a flow loop”, *Energy, Science & Engineering* 2020, vol. 8, pp 1770-1780.
- [18] Christian Stieghorst, Gabriele Hampel, Barbara Karches, Patricia Krenckel, Petra Kudejova, Christian Plonka, Zsolt Revay, Stephan Riepe, Katharina Welter, Norbert Wiehl, “Determination of boron and hydrogen in materials for multicrystalline solar cell production with prompt gamma activation analysis”, *Journal of Radioanalytical and Nuclear Chemistry*, 317 (2018), 307-313.
- [19] Cédric Carasco, Cyrille Eleon, Bertrand Perot, Karim Boudergui, Vladimir Kondrasovs, Gwenolé Corre, Stéphane Normand, Guillaume Sannie, Romuald Woo, Jean-Michel Bourbotte, “Data Acquisition and Analysis of the UNCOSS Underwater Explosive Neutron Sensor”, *IEEE Transactions on Nuclear Science*, Vol. 59, Issue 4, pp 1438-1442, Aug. 2012.
- [20] IAEA Radiation Technology Reports No. 1, Neutron Generators for Analytical Purposes, ISSN 2225-8833, ISBN 978-92-0-125110-7, p. 11.
- [21] Zsolt Revay, Petra Kudejova, Krzysztof Kleszcz, Stefan Soellradl, Christof Genreith, “In-beam activation analysis facility at MLZ, Garching”, *Nuclear Instruments and Methods A*, 799 (2015), 114-123.
- [22] Heinz Maier-Leibnitz Zentrum et al. (2015) “*NECTAR: Radiography and tomography station using fission neutrons*”, *Journal of large-scale research facilities*, 1, A19.

- [23] TH Randriamalala, M Rossbach, E Mauerhofer, Zs Révay, S Söllrad, FM Wagner, “FaNGaS: a new instrument for (n, n’, gamma) reaction measurements at FRM II” (note that FRM II and MLZ are the same facility), Nuclear Instruments and Methods A806:370-377 (2016).
- [24] V. Ullas, D. Kumar and P. K. Roy, "*Epoxy-Glass microballoon syntactic foams: rheological optimization of the processing window*", Hindawi, Advances in Polymer Technology, Vol. 2019, Article ID 9180302, 12 pages (2019).
- [25] USGS 2014 Science for a Changing World Review on International Gas Hydrate.
- [26] H. Gerstenberg, W. Petry, FRM II (20 MW Germany), Encyclopedia of Nuclear Energy, 2021, 113-123.
- [27] Révay Zs., Belgya T. and Molnár G., "*Application of Hypermet-PC in PGAA*", Journal of Radioanalytical and Nuclear Chemistry, Vol. 265 (2005), pp.261-265.

Half pipe configurations	H/C ratio	H (cts/s)
Half pipe alone: no sample	46	0.7
Half pipe with hydrocarbon (1.5 h)	169	3.4

Table 1: H/C intensity ratios and hydrogen peak intensities as measured in the half pipe (the relative uncertainties are lower than 10%).

Samples (first sample comes first in the neutron beam)	H/C theoretical	H/C measured
Rubber	1.18	1.16
Rubber + steel attenuator	1.18	1.04
Water + Rubber	$\gg 1.18$	3.00
Oil + Rubber	> 1.18	1.22
Oil + Water	> 2	2.01
Water + Oil	$\gg 2$	16.7
Water + NaCl solution + Oil + steel attenuator	$\gg 2$	5.9

Table 2 : Theoretical and measured H/C peak area ratios (the relative uncertainties are lower than 10%).



Figure 1 : Hydrate plug extracted from a pipeline [10], [11].

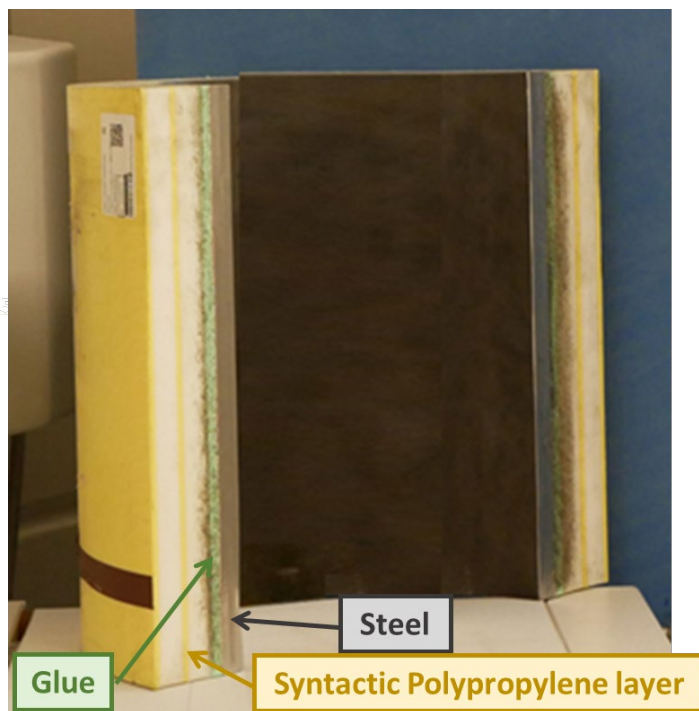


Figure 2: The half-pipe.

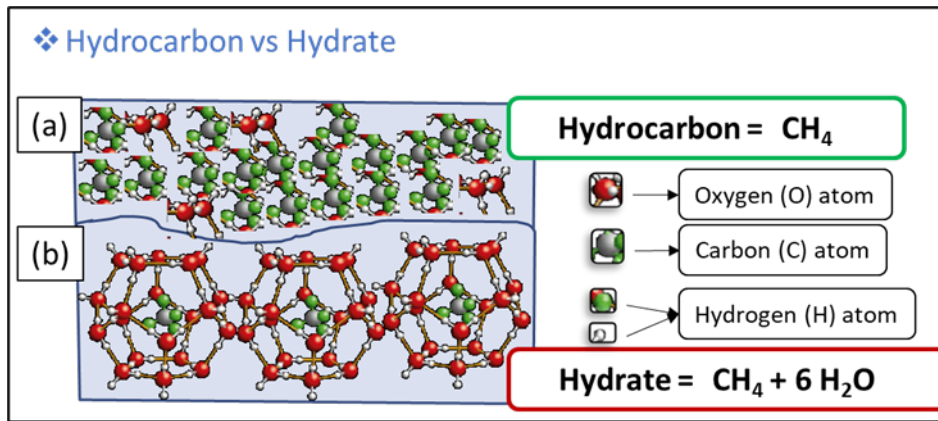


Figure 3: (a) Hydrocarbon phase with a few water molecules, (b) Hydrate phase: H_2O ice cages with trapped hydrocarbon molecules inside them [25].

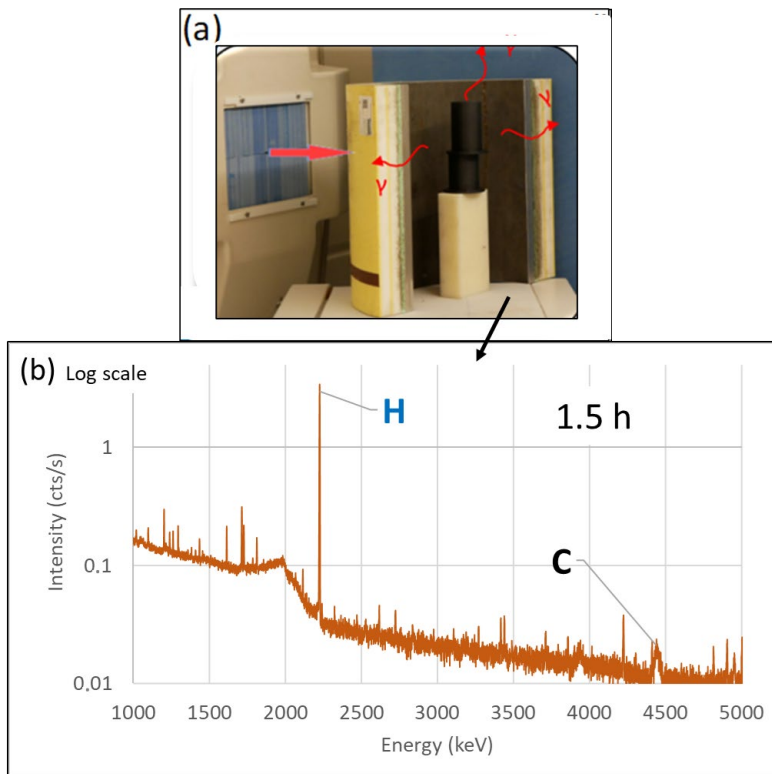


Figure 4: The setup at the FaNGaS instrument

- (a) black hat-shaped PE sample in the center of the half pipe (collimation $5 \times 10 \text{ mm}^2$),
 (b) Gamma spectrum taken for 1.5 h in setup (a) with narrow H peak and broad C peak

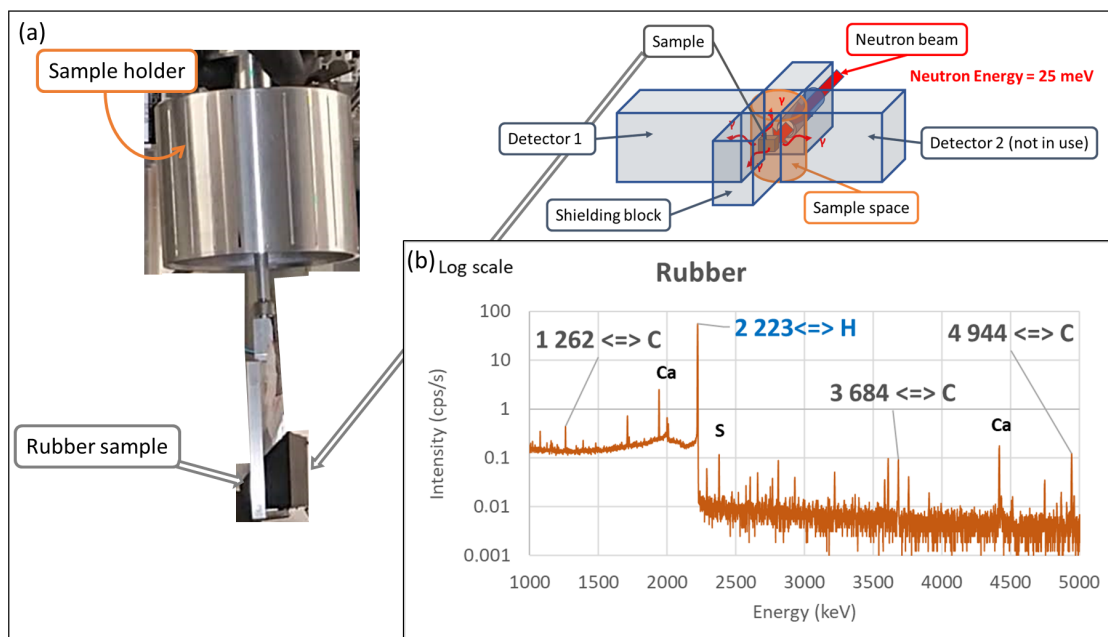


Figure 5: PGAA experiments: (a) The sample holder and the experimental setup, (b) PGAA spectrum of the rubber sample.

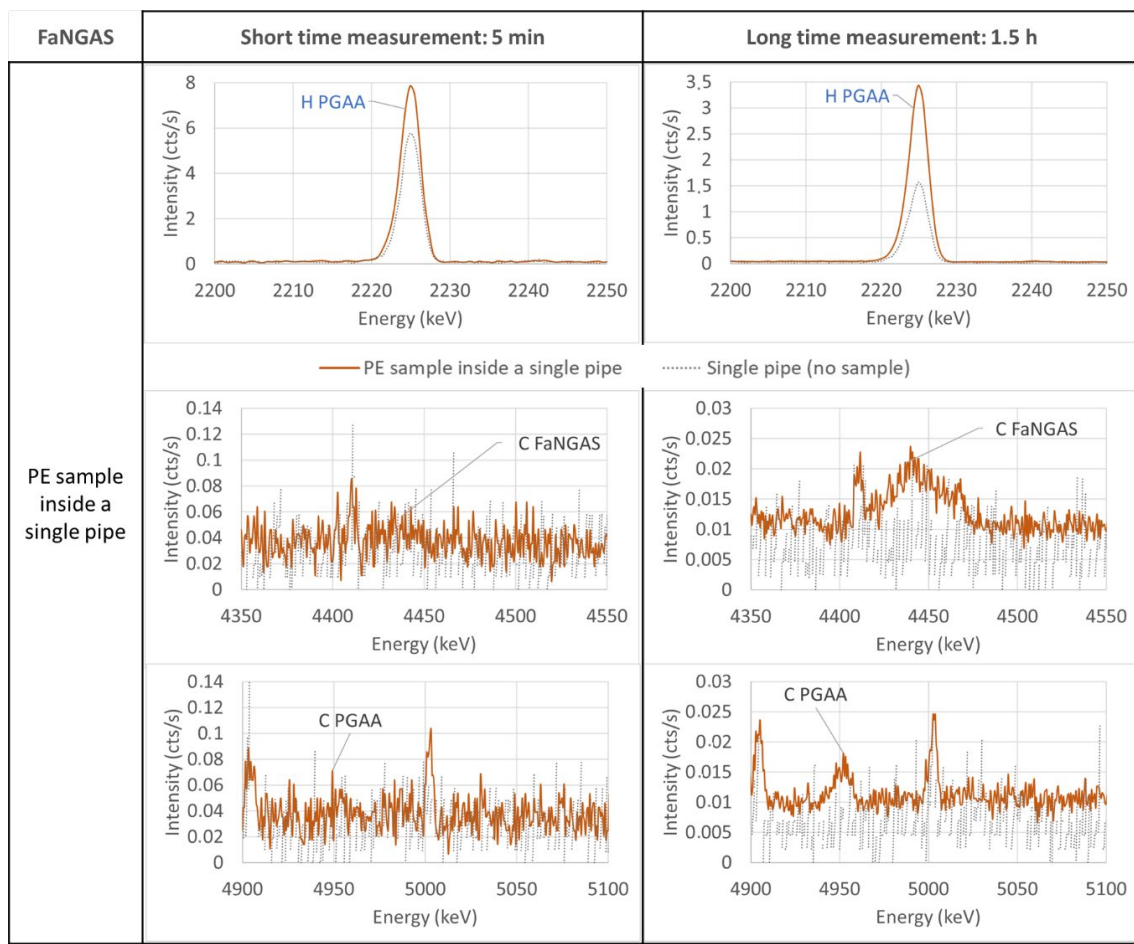


Figure 6: Hydrogen and carbon peaks in gamma spectra for a black hat-shaped PE sample in the center of the half pipe (note that peak intensities are shown in counts per second, i.e. normalized with time; the smaller count rate needs a longer measurement time).

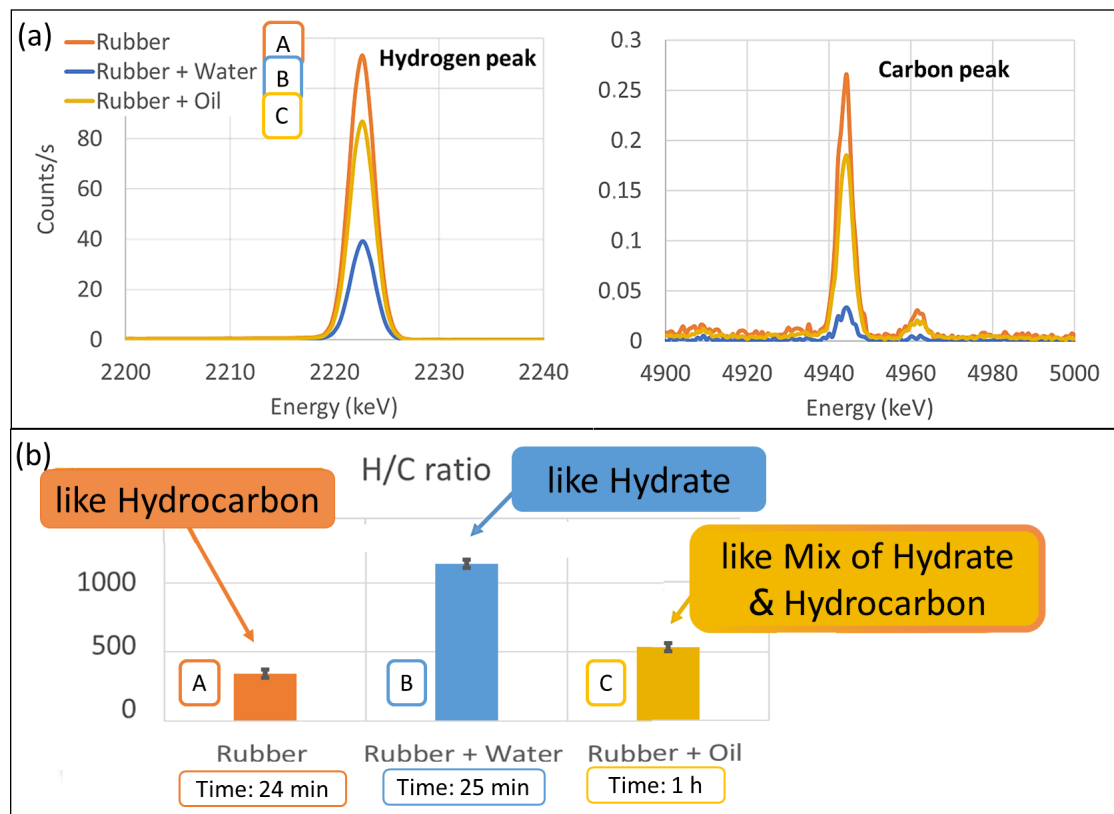


Figure 7: (a) PGAA spectra with H and C peaks highlighted for experiments A, B & C; (b) H/C intensity ratios for comparison between experiments A, B & C.

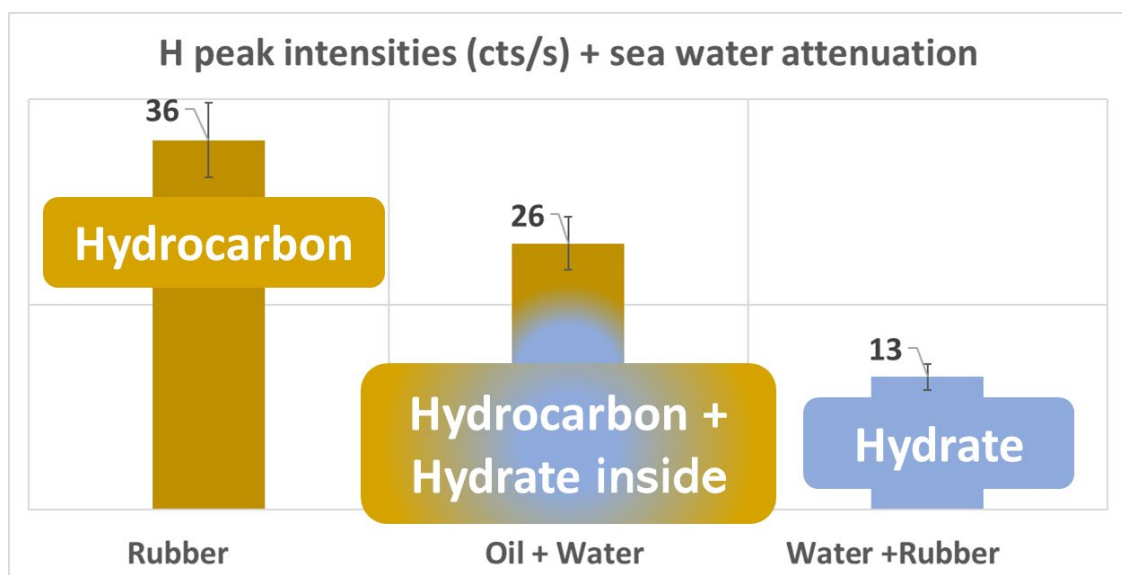


Figure 8: Hydrogen peak intensities from different sample configurations measured with salty water added in the neutron beam path to account for sea water attenuation.